Supplementary Information

Amphoteric Natural Starch-Coated Polymer Nanoparticles with Excellent Protein Corona-Free and Targeting Properties

Bo Huang, ‡[a] Zhenxing Yang, ‡[a] Senbiao Fang, [c] Yan Li, [a] Zicheng Zhong, [a] Ruoqian Zheng, [c] Jinzhi Zhang, [a] Hangxing Wang, [a] Suxiao Wang,[a] Qichao Zou*[a] and Limin Wu*[b]*

[a.] *Ministry of Education Key Laboratory for the Synthesis and Application of Organic Functional Molecules, Hubei Collaborative Innovation Centre for Advanced Organic Chemical Materials, College of Chemistry and Chemical Engineering, Hubei University, Wuhan, 430062, China.*

[b.] *Department of Materials Science and State Key Laboratory of Molecular Engineering of Polymers, Fudan University, Shanghai 200433, China.*

[c] *School of computer science and engineering, Central South University, Changsha, 410012, China.*

‡ *These two authors contributed equally to this work.*

S1.1. Materials

Methyl methacrylate (MMA), acrylic acid (AA), styrene (S), and Iron (II) sulfate heptahydrate ($FeSO_4$ $7H_2O$) (AR 99 %) were all purchased from Macklin. Hydrogen peroxide solution (H_2O_2), fluorescein (AR 99 %) and Tetrakis(para-hydraoxylphenyl) porphyrin (TPPOH) was purchased from Aladdin.

S1.2. Detection of antibodies on nanoparticle surface by flow cytometry.

To detect complete mouse IgG or anti-CD44 on the nanoparticle surface, the IgG conjugated nanoparticles or anti-CD44 conjugated NPs was incubated with anti-mouse IgG-FITC antibodies (Sino Biological) at room temperature for 60 min. Then the free anti-mouse IgG-FITC were washed out by centrifugation purification process. Then, all washed NPs solutions were filled up to 0.5 mL with PBS buffer. Laser power was 50 mW for better nanoparticle detection in flow cytometry. Nanoparticles were displayed in a dot plot at which the SSC and FL1 channel were scaled logarithmically. To obtain the accurate data from constant flow, the samples were recorded at 30 s after the flow started. Quantification of FITC-negative or FITC-positive nanoparticles was performed by defining unconjugated nanoparticles as gate signals.

S1.3. Chemical attach the antibody on as-synthesised starch nanoparticles.

To activate the nanoparticles, the starch-coated NPs were diluted to a concentration of 5 mg mL^{-1} in MES buffer (50 mM, pH 6.1), followed by addition of 6.5 mg (0.03 mmol) of NHS-sulfo and 1.15 mg (0.006 mmol) of EDC-HCl, and then shaken at 250 rpm at room temperature for 1 h. After then, the reaction mixture was washed three times with MES buffer by centrifugation at 10,000 rpm to remove the unreacted material, and diluted to a final volume of 1 mL. 100 μL of the NHS-activated particles dispersion was diluted with 4 mL of MES buffer. 50 μL of anti-CD44 (1.0 mg ml^{-1}) (Sino Biological) or 2 μL of mouse IgG (6 mg mL^{-1}, Jackson) was dissolved in 4 mL of MES buffer and the nanoparticle dispersion was added dropwise to the antibody solution. Finally, this mixture was shaken at room temperature for 4 h and washed three times with PBS by centrifugation at 10,000 rpm. The final volume of the dispersion was adjusted to 3.0 mL.

S1.4. Protein corona-free property.

SDS PAGE method was also used to determine the protein corona free properties. 1mg of pure nanoparticles was incubated with 30% FBS at 37℃for 1 h. Purification of nanoparticles was performed as above. The nanoparticle-protein complex was separated and denatured by boiling for 5 min in loading buffer (Coolaber 3 × protein loading buffer with DTT), and then separated by size in the moiety of porous 10 % polyacrylamide gel (1D SDS-PAGE), in an electric field using a Mini-PRO4 electrophoresis system from WIX. The electrophoresis was run under constant voltage (120 V, 80 min). The gels were stained using silver stain (Beyotime) for 2 h, followed by destaining overnight in deionized water.

Protein corona-free property was also determined by Octed RED96 instrument (FortéBio Biolayer Interferometry, Pall Life Science). The final volume for all the solutions was 200 μL per well. Assays were performed at room temperature in solid black 96-well plates (Geiger Bio-One). Aminopropyl Silane Biosensors (APS) were pre-wetted in PBS buffer for 900 s. 10 % Serum in PBS buffer was loaded onto the surface of APS biosensors for 300 s. A 60 s biosensor baseline step was applied before the analysis of association of the proteins in FBS on the biosensor. The biosensors were balanced in the PBST buffer (PBS/ Tween 20 (0.002%)). SCMMA, SCMM, SCS, SCMMA-AA29 % and SCMMA-fluorescein NPs were diluted to 0.1mg / mL and associations were applied for 175 s.

Protein corona-free property was further determined by Surface Plasmon Resonance (SPR) (Nicoya, Canada). The SPR COOH-sensor chips (Nicoya, Canada) was first stabilized with a PBS solution for 8 min and active by sodium acetate, and then covalently immobilized by 10 % FBS in PBS buffer by the EDC/NHS chemistry. The sensor chips were balanced in PBS buffer and the extra active groups on the chips were blocked by ethanolamine hydrochloride. SCMMA NPs and SCMMA-AA29 % NPs were diluted to 0.1mg / mL and associations were applied for 210 s. In each cycle, a 250 μL sample was flowed through the chip for 5 min at a constant flow rate of 20 μl/min.

S1.5. Targeting property determination.

The hydrodynamic diameters of the antibody conjugated nanoparticles labelled with secondary antibody and the antibody conjugated nanoparticles incubation with FBS and then labelled with secondary antibody were measured by DLS and compared. In addition, the IgG conjugated nanoparticles or anti-CD44 conjugated nanoparticles were incubated in 30 % FBS at 37℃ for 1 h and then incubated with anti-mouse IgG-FITC antibodies (Sino Biological) at room temperature for 60 min. The flow cytometry data was measured to quantify the FITC-negative and FITC-positive nanoparticles. Moreover, FortéBio BIL was also used to determine the targeting properties. CD44 proteins were incubated with biotin for 30 min and washed to eliminate the extra biotin by a gravity desalination column. Biotinylated CD-44 (0.25μg / μL) was loaded onto the Streptavidin capture biosensors (SA), and then the baseline was measured in PBS/ Tween 20 (0.002%) (PBST) buffer. The associations were measured for 170 s in the wells containing SCMMA−anti-CD44 NPs in buffer solution and SCMMA−anti-CD44 NPs in FBS solution. The dissociations were measured in PBST buffer for 500 s. Different concentrations of SCMMA−anti-CD44 NPs (0.1 mg/mL, 0.075 mg/mL, 0.05 mg/mL, 0.025 mg/mL, 0.0125 mg/mL) were applied to repeat the same process using Octed RED96 instrument

S1.6. The Calculation of degree of substitution (DS).

DS of etherified starch was calculated as follows:[1]

$$N\% = \frac{14DS}{162 + 117\,DS}$$

Where N% is the content of nitrogen in the starch which can be derived from elemental analysis ((Elementar vario MICRO CUBE); 14 is the molecular mass of nitrogen; 162 is the molecular mass of dehydrated glucose residue; 117 is the molecular mass of the substitution group. So, DS can be calculated as:

$$DS = \frac{162N}{1400 - 117\,N}$$

S1.7. The calculation of grafting efficiency.

NPs synthesized from starch (ω_1) and monomer (ω_2) were fully dissolved into ethyl acetate under condensation circumstance for three days, in which all of the polymers were dissolved while free starch and starch grafted polymer were insoluble with the mass (ω_3) weighed after freeze drying. Then the starch and starch grafted polymer were dissolved into water under condensation circumstance for three days, in which all the ungrafted starch was dissolved in water while the starch grafted polymer was insoluble with the mass (ω_4) weighed after freeze drying. Assuming all of the monomers have been well polymerized, then the grafted efficiency of polymers (GE_P) can be calculated by $GE_P = (\omega_3 - \omega_1)/ \omega_2$ and are 25.7, 40.9 and 47.6 % for SCS and SCMM and SCMMA NPs, respectively. And the grafted efficiency of starch (GE_S) can be calculated by $GE_S = [\omega_4 - (\omega_3 - \omega_1)]/ \omega_1$, and are 35.9, 35.4 and 33.52 % for SCS and SCMM and SCMMA NPs, respectively. The lowest GE_P for SCS indicates the loosest entangling of starch chains on SCS NPs.

S1.8. The density of outermost shell of NPs.

The density of outermost shell of NPs were calculated by using the average mass (M_1) of single NP, subtract the average mass (M_2) of outershell removed single NP and divide the average volume (V_{shell}) of single NP outermost shell. The average mass of single NP was calculated by using the total mass per unit volume (M_{total}) divide by the number of NPs per unit volume (N) (derived from Flow NanoAnalyzer analysis).

S1.9. The number of antibodies per NPs.

The number of antibodies per NPs were calculated by using the number of the conjugated antibodies on the unit volume of NPs solution ($N_{antibody}$) divided the number of NPs per unit volume (N_{np}). $N_{antibody}$ was derived from the mass of antibodies ($M_{antibody}$) dividing the molecular weight of antibody ($MW_{antibody}$) and converted to $N_{antibody}$ by applying Avogadro number. $M_{antibody}$ was derived from the typical Western blot protein quantification method and N_{np} was derived from Flow NanoAnalyzer analysis.

S1.10. Cell viability.

The cytotoxicity of SCMMA NPs was evaluated using a Vybrant® MTT cell Proliferation Assay Kit. Briefly, Hela cells (□5,000 cells per well) were grown in 96-well plate at 37℃ for 24 h under 5% CO_2 condition prior to the experiment. The NPs were diluted into different concentrations (0.5, 0.25, 0.12, 0.06, 0.03, 0.015 and 0.01 mg / mL) with full minimum essential medium (MEM). 100 μL MEM containing SCMMA NPs was incubated with pre-incubated cells in 96 wells at 37℃ for 48 h and 100 μL full MEM medium without NPs was used as the control. Then 20 μL MTT stock solution (5 mg/mL PBS solution) was added in each well and incubated at 37℃for another 4 h. MTT-containing medium was replaced with 150 μL DMSO to dissolve the formed crystal at 37℃ under gentle shaking. Absorbance at 570 nm was measured using a microplate reader (Bio-Rad 550) with DMSO as the blank reading. The cell viability upon NPs treatment was estimated in triplicate: cell viability (%) = 100 × (Abs_{sample} - A_0)/($Abs_{control}$- A_0).

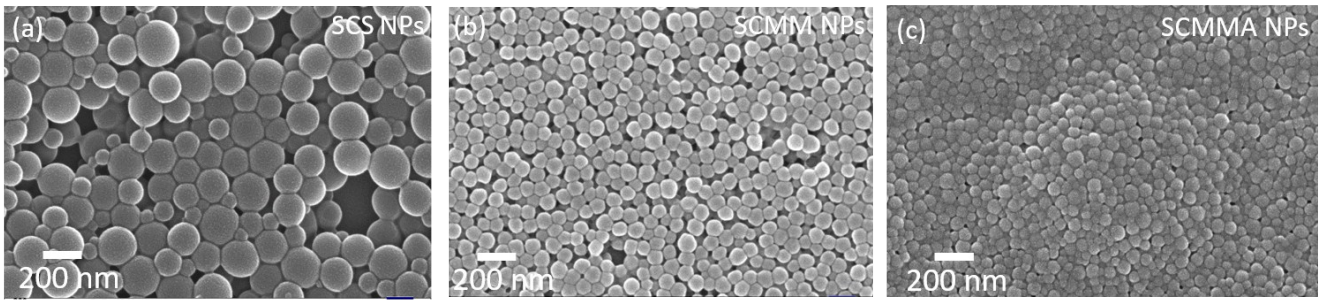

Figrue S1. Typical SEM images of unpurified (a) SCS NPs, (b) SCMM NPs and (c) SCMMA NPs.

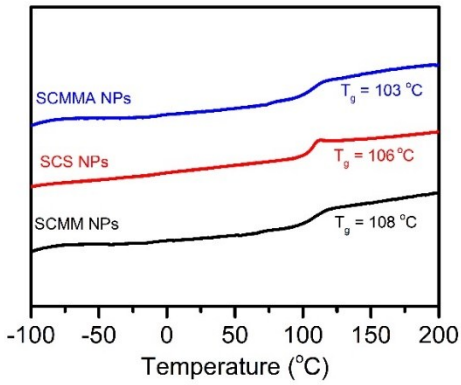

Figure S2. Glass rubber transition temperature (Tg) of SCS, SCMM and SCMMA NPs measured by differential scanning calorimeter (DSC).

(a)

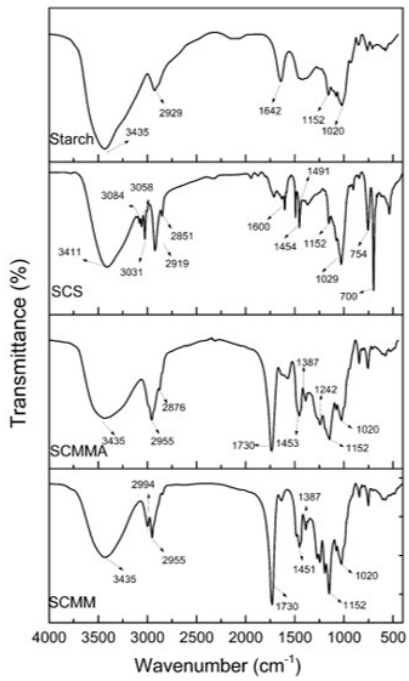

(b)

Starch	MMA	AA	St	SCS	SCMM	SCMMA	Peak assignment
1020	-	-	-	1029	1020	1020	ν_{as}-C–O–C stretching vibrations of the starch
1152	-	-	-	1152	1152	1152	C–O stretching of the Starch
-	1387,2955	-	-	-	1387,2955	1387,2955	$-CH_3$ from MMA
-	-	-	1450~1600, 3000~3100	1450~1600, 3000~3100	-	-	C-H stretching vibration and breathing vibration of benzene ring
-	1730	1730	-	-	1730	1730	–COOH from AA and the -C=O groups from MMA
2929	2876,2955	2876	2851, 2919	2851, 2919	2955, 2994	2876,2955	C–H stretching
3435	-	3435	-	3411	3435	3435	O-H stretching vibration from Starch and the –COOH from AA

Figure S3. (a) FTIR spectra of starch, SCS, SCMMA and SCMM NPs. (b) The relative FIIR spectra of SCS, SCMMA and SCMM NPs after condensation circumstance. (c) Peak assignment of FTIR spectra.

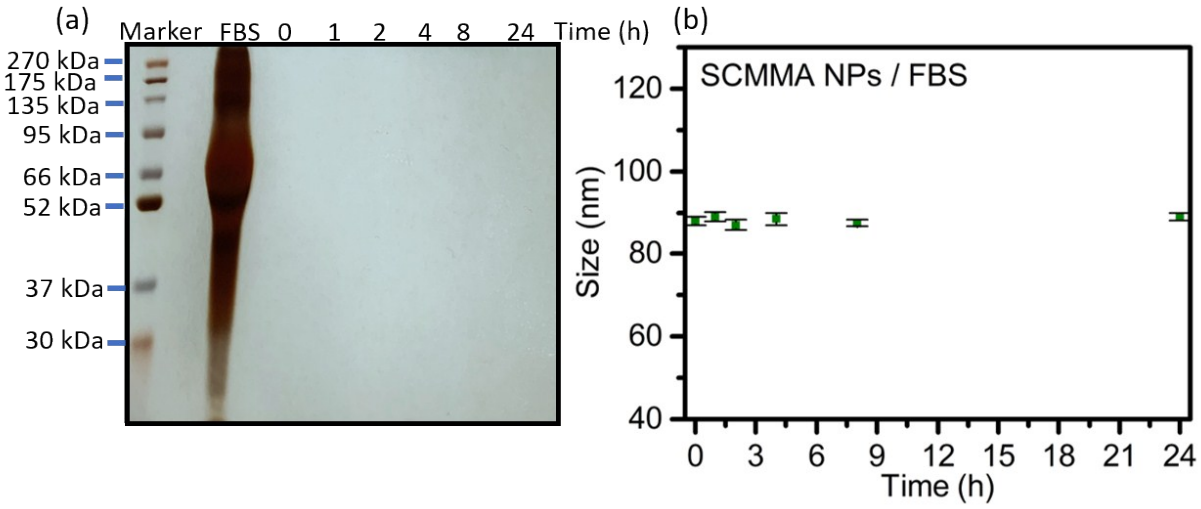

Figure S4. (a) Protein bands from the SDS-PAGE of SCMMA NPs with different FBS incubation time. (b) Mean diameters of SCMMA NPs after FBS treatment under different incubation time.

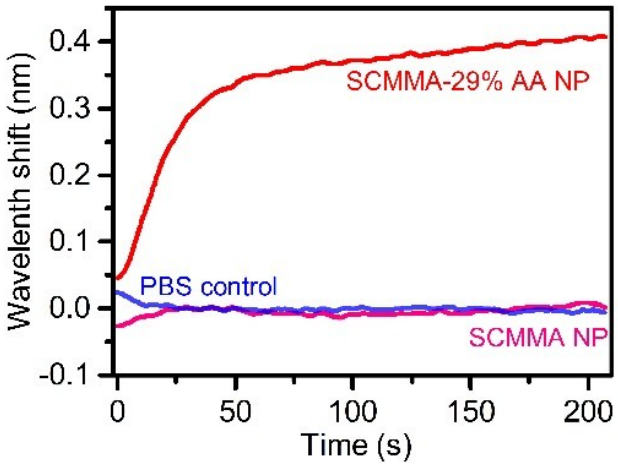

Figure S5.. SPR spectra indicating the low interaction of proteins with SCMMA NPs but a strong interaction with SCMMA-29% AA NPs.

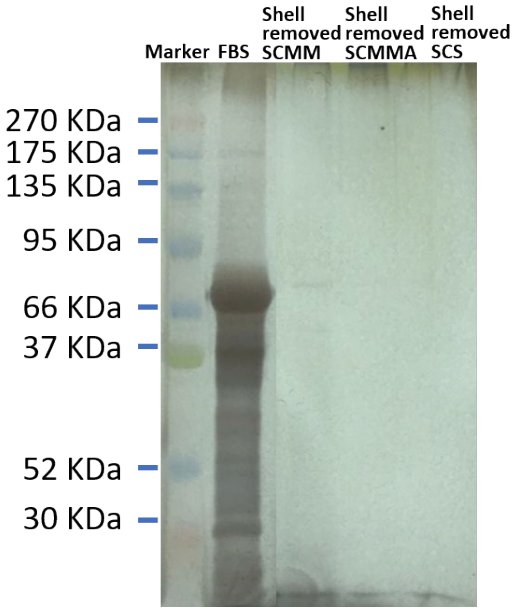

Figure S6. SDS-PAGE gel of the outermost shell-removed SCMM NPs, the outermost shell-removed SCMMA NPs and the outermost shell-removed SCS NPs incubated with 30 % FBS solution.

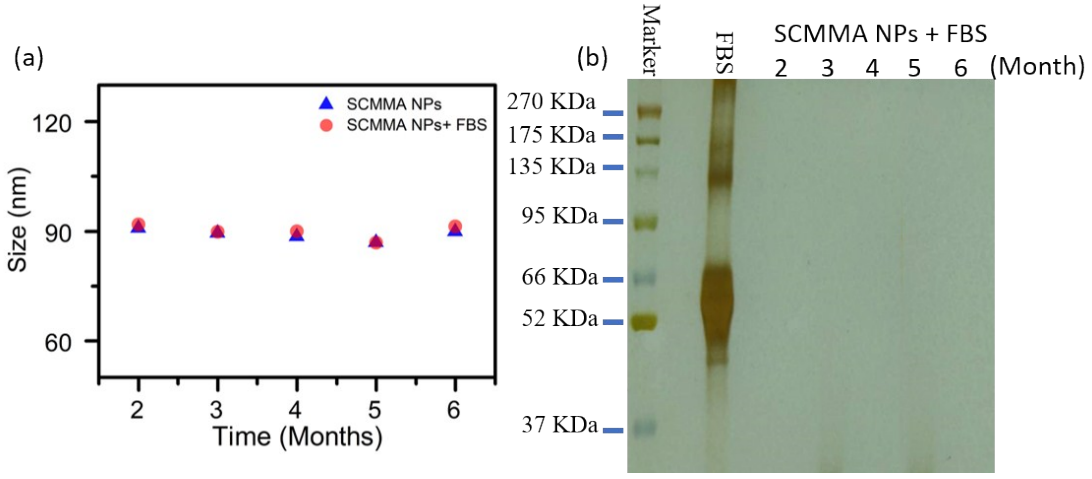

Figure S7. Long-term storage stabilities: (a) Hydrodynamic diameters of SCMMA NPs in PBS (triangle) and in FBS solutions (circle) at different storage time. (b) Protein bands on SDS-PAGE gel of FBS treated SCMMA NPs.

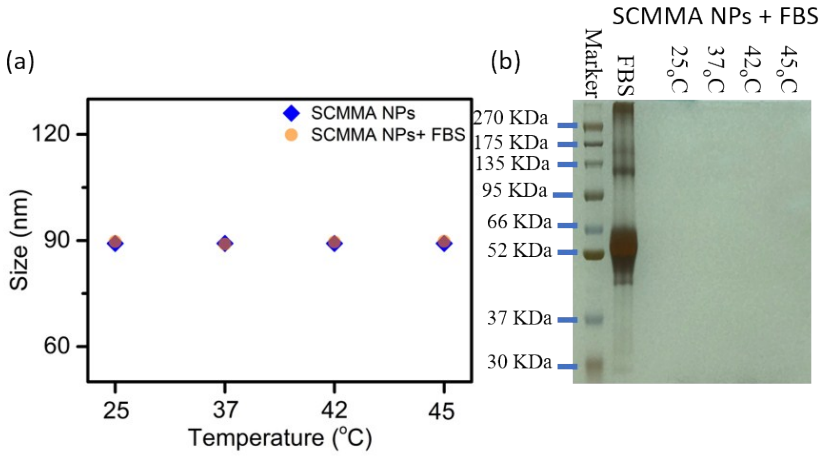

Figure S8. (a) Hydrodynamic diameters of SCMMA NPs in PBS (diamond) and in FBS solutions (circle) at different temperature. (b) Protein bands on SDS-PAGE gel of FBS treated SCMMA NPs at different temperature.

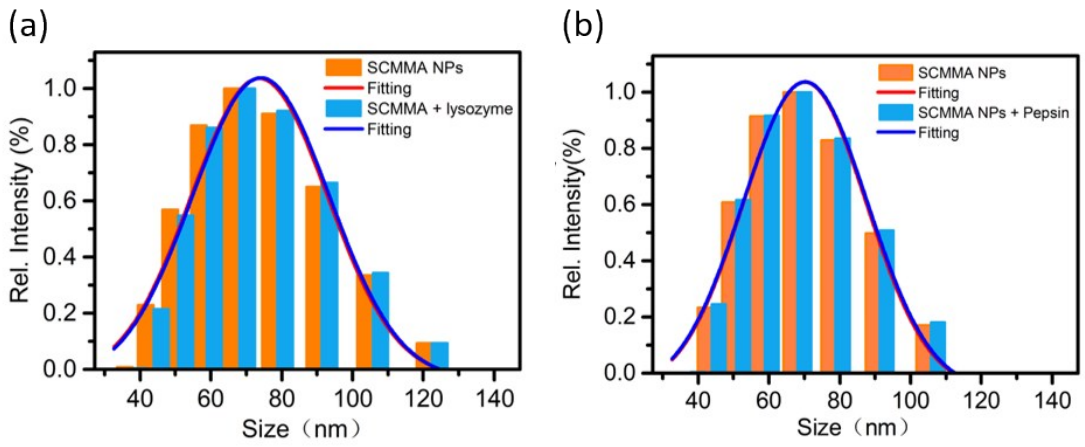

Figure S9. The hydrodynamic sizes of SCMMA NPs before and after incubation with lysozyme (a) and pepsin (b) don't show any shift.

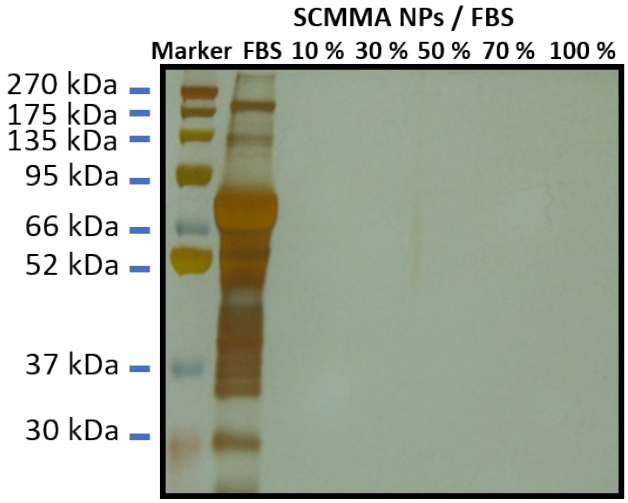

Figure S10. Protein bands indicating the anti-fouling property of SCMMA NPs incubated with 10 % FBS, 30 % FBS, 50 % FBS, 70 % FBS, and 100 % FBS.

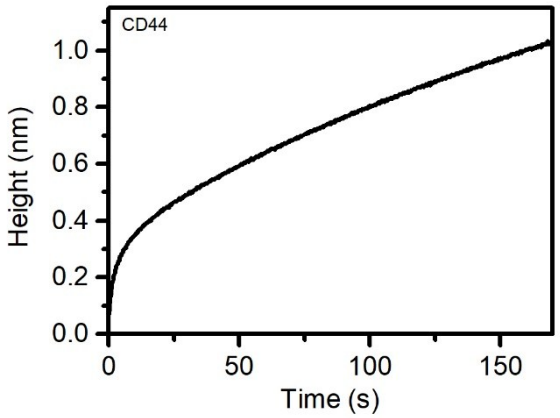

Figure S11. FortéBio BLI scan of biotinylated-CD44 adsorption on streptavidin biosensor. 1 nm interferometry shift indicating the strong binding of CD44 antigen on biosensor.

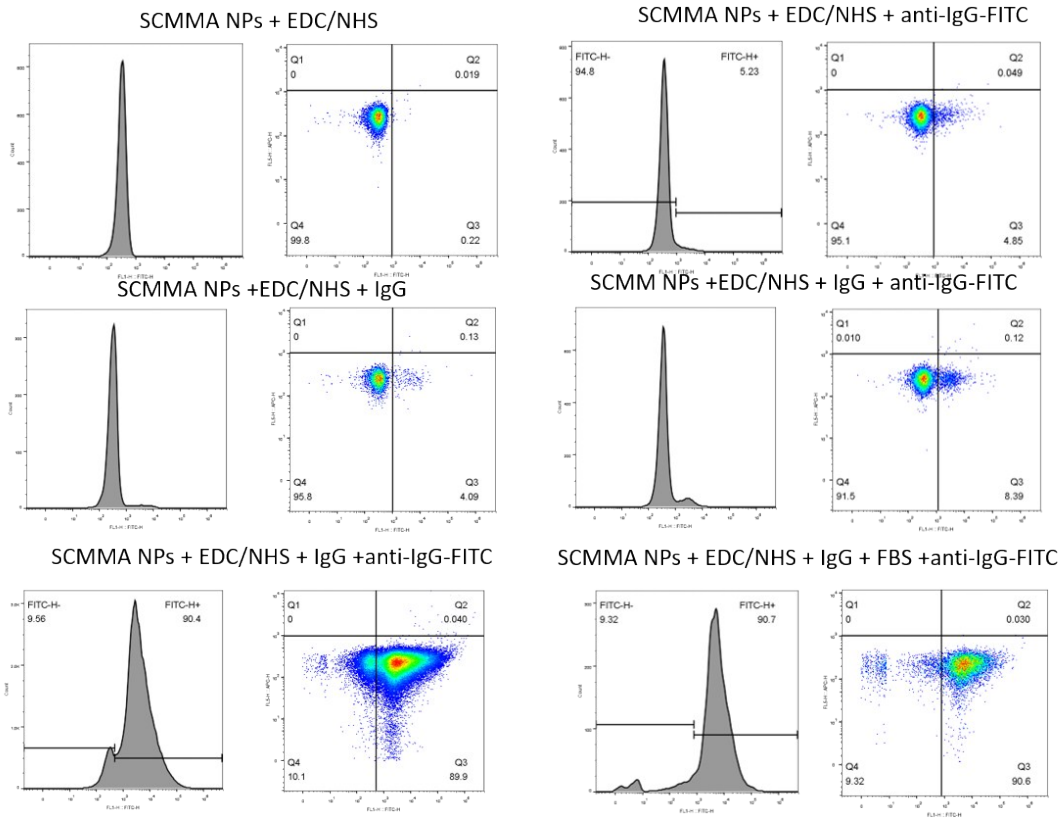

Figure S12. Flow cytometry results shown as the amount of FITC-positive nanoparticles in percentage and for independent experiments (n = 3).

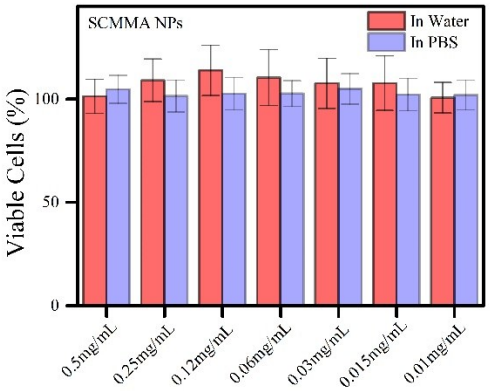

Figure S13. Viability of Hela cells after incubation with various SCMMA NPs concentrations of 0.01 mg / mL to 0.5 mg / mL for 24 h. Red, NPs in water. Blue, NPs in PBS buffer.

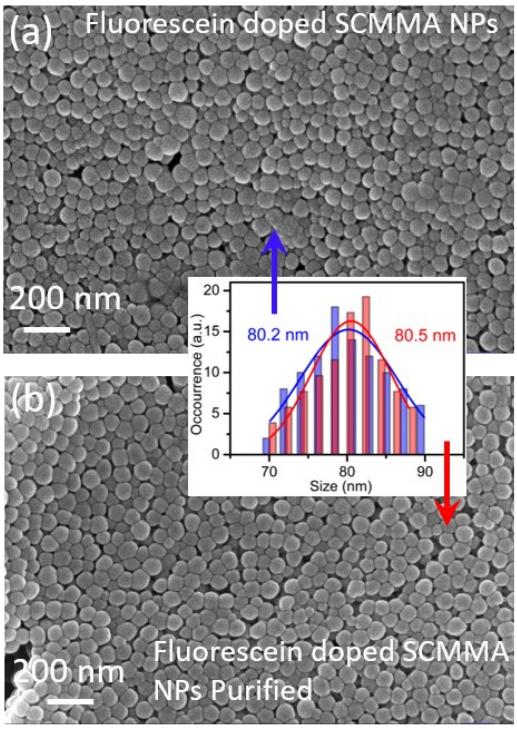

Figure S14. Typical SEM images of (a) fluorescein doped SCMMA NPs and (b) purified fluorescein doped SCMMA NPs indicate their similar sizes and shape. Inset, NPs sizes distributions from SEM images.

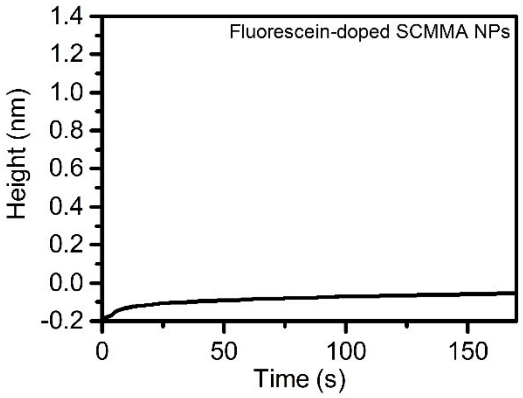

Figure S15. BLI spectrum of the fluorescein-doped SCMMA NPs.

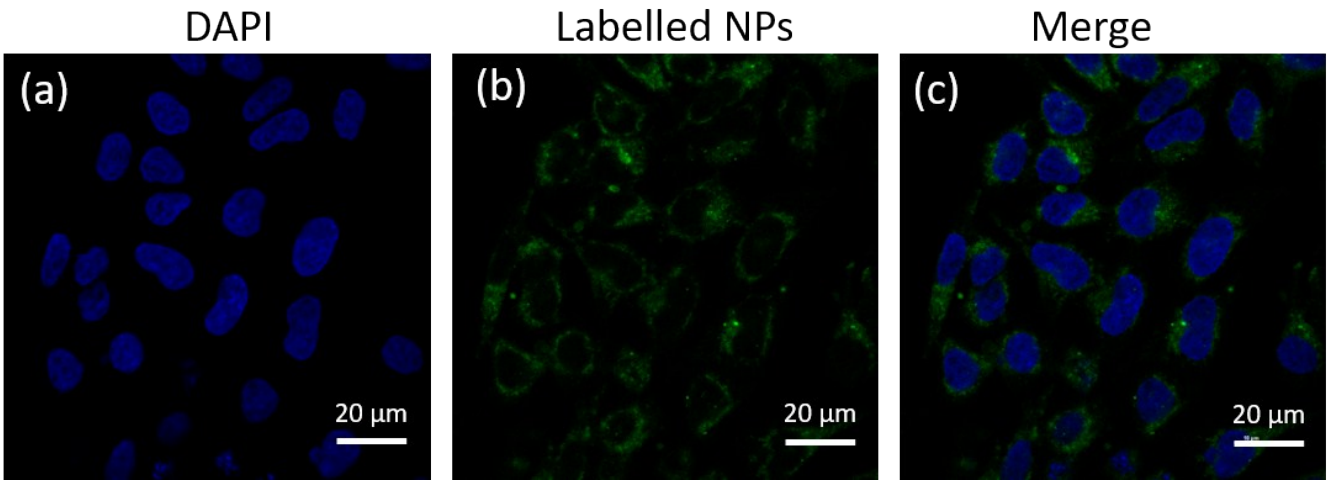

Figure S16. Images of SW480 cells incubated with fluorescein-doped SCMMA NPs.

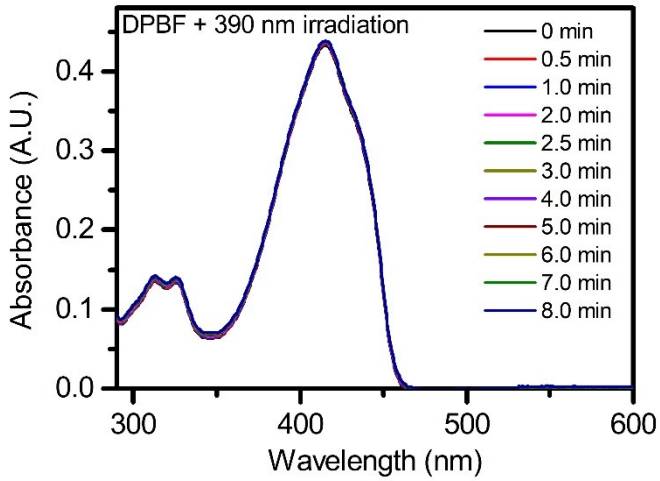

Figure S17. Absorption spectrum of DPBF under 390 nm irradiation with different time .

References

1 M. Khalil, A. Hashem, A. Hebeish, *Starch-Stärke* **1990**, *42*, 60-63.